Electronic Supplementary Material (ESI) for Physical Chemistry Chemical Physics.

Supplementary Information

Graphene Networks and Its Role on Free-Volume Properties of Graphene/Epoxidied Natural Rubber Composites with a Segregated Structure: Rheological and Positron Annihilation Studies

Canzhong He [a,b,c], Xiaodong She [b,c,*], Zheng Peng [a,c*], Jieping Zhong[a], Shuangquan Liao[b],
Wei Gong [a], Jianhe Liao[b] and Lingxue Kong [c]

[a] Chinese Agricultural Ministry Key Laboratory of Tropical Crop Product Processing, Agricultural Product Processing Research Institute, Chinese Academy of Tropical Agricultural Sciences, Zhanjiang 524001, PR China

[b] College of Materials and Chemical Engineering, Hainan university, Haikou, 571737, PR China

[c] Institute for Frontier Materials, Deakin University, Waurn Ponds, Geelong VIC 3216, Australia

1. Detail description of experiments

1.1 Preparation of epoxidized natural rubber Latex (ENRL)

Epoxidation of the isoprene unit of the natural rubber (NR) was performed with the reaction between NR and formic acid-hydrogen peroxide system. Briefly, 333.4g of NR latex was stabilized with nonionic surfactant and diluted with distilled water to a total solid content of 30%. 19.5g formic acid

---

[*] Corresponding authors. Tel: +61 416 462 459. E-mail: xiaodongshe@icloud.com (Xiaodong She), zpengcatas@126.com (Zheng Peng)

and 150g hydrogen peroxide were then slowly added into the NR latex under mechanical stir. The reaction was carried out for 10 h at 50 °C to obtain ENR latex. The molar percentage of epoxy groups (25 mol%), and hydroxyl groups (3.8 mol%) were determined with FT-IR method [1].

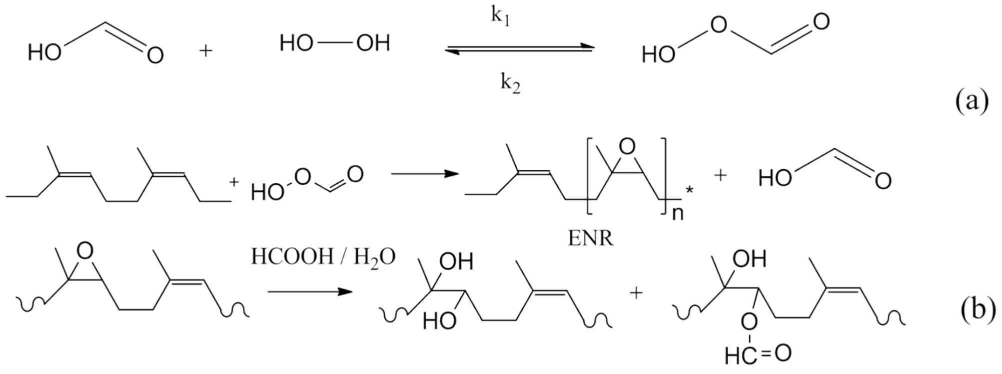

Schematic indication of the reaction mechanism of epoxidized double bond by peroxy acids

1.2 Preparation of graphene oxide (GO)

GO was prepared by oxidizing natural graphite powder according to the modified Hummers method [2-3]. The oxidation process was accomplished by treating graphite with concentrated H_2SO_4, $KMnO_4$ $NaNO_3$. The obtained GO was then exfoliated in water via sonication to form 6 mg·ml^{-1} dispersion. The prepared GO/H_2O solution is deposited onto mica wafer for AFM observation to investigate the degree of exfoliation of the GO in water. It is found that GO presents as irregularly shaped sheets with a uniform average thickness of 0.8 nm and a lateral extent of 0.5~4 μm (Fig. S1). This observation indicates GO has been completely exfoliated into individual sheets.

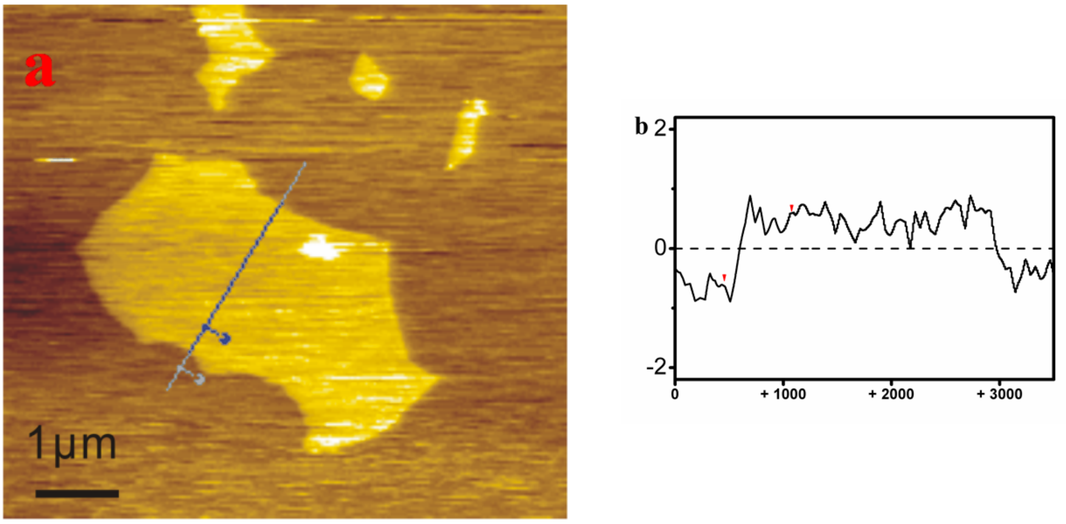

Fig. S1- AFM image of GO sheets (a) topograph, (b) height profile

2. Positron Annihilation Lifetime Spectroscopy (PALS) data analysis

2.1 Mean Free-Volume Hole Size and Fraction

Positron lifetime spectra were best fitted with three components using PATFIT [4]. The shortest-lived component τ_1 (~0.15 ns) is attributed to the self-annihilation of *para*-positronium and "free" positron annihilation. The intermediate-lived component, τ_2=0.40±0.02 ns, is assigned to annihilation of positron trapped in various vacancies. The longest-lived component, τ_3, is attributed to the o-Ps pick-off annihilation in free-volume holes in amorphous region. According to the simplified free-volume model, the average radius R of free-volume holes can be evaluated from τ_3, as described in eq 1[5]

$$\tau_{o-Ps} = \frac{1}{2}\left[1 - \frac{R}{R+\Delta R} + \frac{1}{2\pi}\sin\left(\frac{2\pi R}{R+\Delta R}\right)\right]^{-1} \qquad (1)$$

Where $\tau_{o\text{-}Ps}$ represents o-Ps lifetime, R is the size of free volume holes and $\Delta R = 1.66Å$ is the fitted empirical electron-layer thickness [6]. The intensity of o-Ps, I_3, is supposed to be linearly dependent on the concentration of freevolume holes. The fractional free-volume F_v can be expressed as $F_v = CI_{o\text{-}Ps}V_f$, where $V_f = (4/3)\pi R^3$ is the average volume of free-volume hole (assuming spherical geometry).

Since only the long-lived o-Ps lifetimes could be related to the properties of the pores in the samples, the following discussions are mainly based on the annihilation characteristics of the long-lived components.

2.2 *Free-Volume Hole Distributions*

Since the free-volume hole exists in a distribution, the o-Ps lifetime is expressed more correctly as a distribution rather than as discrete values. Hence, we employ the expression of positron lifetime spectra in the form:

$$\mathrm{N(t)} = \int_{0}^{\infty} \lambda\alpha(\lambda)e^{-\lambda t}\, d\lambda + \mathrm{B} \qquad (2)$$

where λ (the annihilation rate) is the reciprocal of lifetime τ with an annihilation probability-density function *λa,* and *B* is the background of the spectrum. The computer program CONTIN [7] was employed to provide *λa* vs *λ* for a PAL spectrum by using the measured reference spectrum in Cu (τ= 122 ps). Following the correlation between τ_3 and the hole radius *R* (eq 1), considering the difference of o-Ps capture probability in different hole sizes with a linear correction *K(R)*=1+ *8R,* and using a spherical approximation of free-volume holes, the free-volume probability-density function, $\mathrm{V_f}$(pdf), is expressed as [8-9]

$$\mathrm{V_f(pdf)} = -3.32\left\{\cos\left[\frac{2\pi\mathrm{R}}{\mathrm{R}+1.66}\right]-1\right\}\alpha(\lambda)/\{(\mathrm{R}+1.66)^2K(R)4\pi R^2\} \qquad (3)$$

The fraction of hole volume between $\mathrm{V_f}$ and $\mathrm{dV_f}$ is $\mathrm{V_f}$(pdf)$\mathrm{dV_f}$.

2.3 *Positron age momentum correlation (AMOC) measurements*

The AMOC measurements were performed by acquiring positron lifetime and Doppler broadening radiation spectra in coincidence. The correlated events were recorded using a multi-parameter acquisition system. In the present experiments, positron age dependent Doppler broadening spectra were obtained by summing the correlated events within a variable window (t_1 to t_2) on the positron age axis. The positron age dependent Doppler broadening spectra were analyzed in terms of the age dependent line shape parameter S(t), $t = (t_1 + t_2)/2$, which is determined as the ratio of central area (511 ±1.2 keV) to the total area of the photo peak. There is only one positron component (390 ps) from annihilation of positrons in the source and was ignored in the evaluation of S(t).

3. Electrical conductivity of the graphene-filled rubber composites

Currently, electrically conductive graphene-filled rubber composites are mainly fabricated via solution mixing or in-situ reduction based latex compounding. Some representative results were listed in Table S1.

Table S1 Electrical conductivity of the graphene-filled rubber composites

Matrix	Fabrication method	Percolation threshold (vol.%)	Conductivity (vol.%)	Refs.
SBS[a]	Solution blending	0.12	1.64×10^{-2} S/m at 2.0	[10]
PDMS[b]	Solution blending	0.63	$\approx 2.0 \times 10^{-5}$ S/m at 0.15	[11]
S-SBR[c]	Internal mixer and two roll mixing	≈6.24	$\approx 1.0 \times 10^{-5}$ S/m at 20.80	[12]
SBR	Latex hetero-coagulation	≈0.41	8.24×10^{-4} S/m at 2.08	[13]
NR	Solution blending	≈0.41	≈0.01 S/m at 2.08	[14]
NR	Self assembly in latex	0.62	≈0.5 S/m at 8.30	[15]
NR	Self-assembly integrating latex compounding	0.21	7.31 S/m at 4.16	[16]
ENR	Solution blending	0.23	7.7 S/m at 3.36	Present work

[a] Styrene – butadiene – styrene.

[b] Polydimethylsilicone.

[c] Solution styrene butadiene rubber.

References

[1] Yu HP, Zeng ZQ, Lu G, Wang QF. Processing characteristics and thermal stabilities of gel and sol of epoxidized natural rubber. European Polymer Journal. 2008;44(2):453-64.

[2] Becerril HA, Mao J, Liu Z, Stoltenberg RM, Bao Z, Chen Y. Evaluation of solution-processed reduced graphene oxide films as transparent conductors. ACS Nano. 2008;2(3):463-70.

[3] Hirata M, Gotou T, Horiuchi S, Fujiwara M, Ohba M. Thin-film particles of graphite oxide 1: High-yield synthesis and flexibility of the particles. Carbon. 2004;42(14):2929-37.

[4] Kirkegaard P, Eldrup M, Mogensen OE, Pedersen NJ. Program system for analysing positron lifetime spectra and angular correlation curves. Computer Physics Communications. 1981;23(3):307-35.

[5] Tao SJ. Positronium annihilation in molecular substances. The Journal of Chemical Physics. 1972;56(11):5499-510.

[6] Nakanish H, Wang SJ, Jean YC. World Science: Singapore. 1988:292.

[7] Gregory RB, Zhu Y. Analysis of positron annihilation lifetime data by numerical laplace inversion with the program CONTIN. Nuclear Inst and Methods in Physics Research, A. 1990;290(1):172-82.

[8] Deng Q, Jean YC. Free-volume distributions of an epoxy polymer probed by positron annihilation: Pressure dependence. Macromolecules. 1993;26(1):30-4.

[9] Liu J, Jean YC, Yang H. Free-volume hole properties of polymer blends probed by positron annihilation spectroscopy: miscibility. Macromolecules. 1995;28(17):5774-9.

[10] Li H, Wu S, Wu J, Huang G. Enhanced electrical conductivity and mechanical property of SBS/graphene nanocomposite. Journal of Polymer Research. 2014;21(5).

[11] Fakhru'l-Razi A, Atieh MA, Girun N, Chuah TG, El-Sadig M, Biak DRA. Effect of multi-wall carbon nanotubes on the mechanical properties of natural rubber. Composite Structures. 2006;75(1-4):496-500.

[12] Das A, Kasaliwal GR, Jurk R, Boldt R, Fischer D, Stöckelhuber KW, et al. Rubber composites based on graphene nanoplatelets, expanded graphite, carbon nanotubes and their combination: A comparative study. Composites Science and Technology. 2012;72(16):1961-7.

[13] Kim JS, Hong S, Park DW, Shim SE. Water-borne graphene-derived conductive SBR prepared by latex heterocoagulation. Macromolecular Research. 2010;18(6):558-65.

[14] Prud'Homme R, Ozbas B, Aksay I, Register R, Adamson D. Functional graphenerubber nanocomposites. Google Patents;2010.

[15] Zhan Y, Lavorgna M, Buonocore G, Xia H. Enhancing electrical conductivity of rubber composites by constructing interconnected network of self-assembled graphene with latex mixing. Journal of Materials Chemistry. 2012;22(21):10464-8.

[16] Luo Y, Zhao P, Yang Q, He D, Kong L, Peng Z. Fabrication of conductive elastic nanocomposites via framing intact interconnected graphene networks. Composites Science and Technology. 2014;100:143-51.